

Reconstitution and Characterization of the *Vibrio cholerae* Vibriobactin Synthetase from VibB, VibE, VibF, and VibH[†]

Thomas A. Keating,[‡] C. Gary Marshall,[‡] and Christopher T. Walsh*

Department of Biological Chemistry and Molecular Pharmacology, Harvard Medical School, Boston, Massachusetts 02115

Received July 14, 2000; Revised Manuscript Received September 20, 2000

ABSTRACT: Vibriobactin [*N*¹-(2,3-dihydroxybenzoyl)-*N*⁵,*N*⁹-bis[2-(2,3-dihydroxyphenyl)-5-methyloxazolinyl-4-carboxamido]norspermidine], is an iron chelator from the cholera-causing bacterium *Vibrio cholerae*. The six-domain, 270 kDa nonribosomal peptide synthetase (NRPS) VibF, a component of vibriobactin synthetase, has been heterologously expressed in *Escherichia coli* and purified. VibF has an unusual NRPS domain organization: cyclization–cyclization–adenylation–condensation–peptidyl carrier protein–condensation (Cy₁–Cy₂–A–C₁–PCP–C₂). VibF activates and covalently loads its PCP with L-threonine, and together with vibriobactin synthetase proteins VibE (adenylation) and VibB (aryl carrier protein) condenses and heterocyclizes 2,3-dihydroxybenzoyl–VibB with L-Thr to 2-dihydroxyphenyl-5-methyloxazolinyl-4-carboxy–VibF in the first demonstration of oxazoline formation by an NRPS cyclization domain. This enzyme-bound aryl oxazoline can be transferred by VibF to various amine acceptors but most efficiently to *N*¹-(2,3-dihydroxybenzoyl)norspermidine (*k*_{cat} = 122 min^{−1}, *K*_m = 1.7 μM), the product of 2,3-dihydroxybenzoyl–VibB, norspermidine, and VibH. This diacylated product undergoes a second aryl oxazoline acylation on its remaining secondary amine, also catalyzed by VibF, to yield vibriobactin. Vibriobactin biosynthesis in vitro has thus been accomplished from four proteins, VibE, VibB, VibF, and VibH, with the substrates 2,3-dihydroxybenzoic acid, L-Thr, norspermidine, and ATP. Vibriobactin synthetase is an unusual NRPS in that all intermediates are not covalently tethered as PCP thioesters and in that it represents an NRPS pathway with two branch points.

Vibriobactin (1) is an iron chelator (siderophore) from the causative agent of cholera, the Gram-negative bacterium *Vibrio cholerae* (1). Iron being a required element for microbial growth, bacteria have evolved systems to scavenge Fe(III) from their environment, particularly the iron-binding proteins of their hosts. These systems encompass the biosynthetic machinery necessary to assemble the small-molecule siderophore, transport pathways to secrete and then reuptake the ferric–siderophore complex, and some means of extracting the scavenged iron from its tightly bound complex. Vibriobactin belongs to the catechol class of siderophores (2), other members of which include enterobactin from *Escherichia coli* (3), anguibactin from *Vibrio*

anguillarum (4), and protochelin from *Azotobacter vinelandii* (5), and with three catechols it is expected to form a 1:1, hexacoordinate complex with Fe(III).

A retrobiosynthesis of vibriobactin (Figure 1) indicates it is composed of three molecules of 2,3-dihydroxybenzoic acid (DHB), two of L-threonine, and one of the unusual polyamine norspermidine [bis(3-aminopropyl)amine] (6, 7). Both threonines are linked to DHB residues and have been cyclized and dehydrated to form 5-methyloxazoline moieties. The two 2-(2,3-dihydroxyphenyl)-5-methyloxazoline-4-carboxamide groups are reminiscent of similar groups of yersiniabactin (8) and pyochelin (9) [[2-(2-hydroxyphenyl)thiazolinyl]-thiazolidine-4-carboxylate] and in particular of mycobactin (10) [2-(2-hydroxyphenyl)oxazoline-4-carboxamide], all of which are siderophores from pathogenic bacteria (*Yersinia pestis*, *Pseudomonas aeruginosa*, and *Mycobacterium tuberculosis*, respectively). All the aforementioned siderophores, as well as a great number of antibiotics and other bioactive compounds, are peptidelike molecules biosynthesized nonribosomally by large, multidomain enzymes termed nonribosomal peptide synthetases (NRPSs) (11). It has become apparent from genetic studies on the biosynthesis of vibriobactin (12, 13) that it, too, arises from an NRPS, albeit a nonstandard example. NRPS products are typically linear or macrocyclized assemblages of peptide monomers, which possess both a carboxylate moiety for thioester attachment to NRPS carrier protein domains and a nucleophilic amine for condensation and chain growth. Product biosyn-

[†] This work has been supported by the National Institutes of Health (Grant AI042738 to C.T.W.). T.A.K. is a fellow of the Cancer Research Fund of the Damon Runyon–Walter Winchell Foundation (DRG-1483). C.G.M. is a postdoctoral fellow of the National Science and Engineering Research Council of Canada.

* To whom correspondence should be addressed: Phone 617-432-1715; fax 617-432-0438; e-mail walsh@walsh.med.harvard.edu.

[‡] These authors contributed equally to this work.

¹ Abbreviations: NRPS, nonribosomal peptide synthetase; PKS, polyketide synthase; CoA, coenzyme A; A, adenylation domain; Cy, cyclization domain; PPTase, phosphopantetheinyl transferase; P-pant, 4-phosphopantetheine; PP_i, inorganic pyrophosphate; ICL, isochorismate lyase; ArCP, aryl carrier protein domain; PCP, peptidyl carrier protein domain; C, condensation domain; DTT, dithiothreitol; TCEP, tris(carboxyethyl)phosphine; TCA, trichloroacetic acid; DHB, 2,3-dihydroxybenzoate; NSPD, norspermidine; DAH, 1,7-diaminoheptane; DHB-NSPD, *N*¹-(2,3-dihydroxybenzoyl)norspermidine; DHB-DAH, *N*-(2,3-dihydroxybenzoyl)-1,7-diaminoheptane.

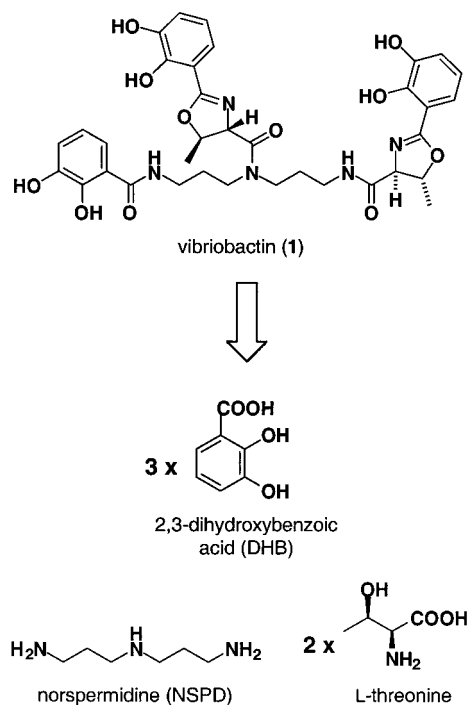


FIGURE 1: *Vibrio cholerae* iron chelator vibriobactin and its retrobiosynthesis into 3 equiv of 2,3-dihydroxybenzoic acid (DHB), 2 equiv of L-threonine, and 1 equiv of norspermidine.

thesis proceeds in an N-to-C direction with amide bond formation between successive pairs of upstream donors and downstream acceptors (14). By contrast, vibriobactin has no free carboxylate that would offer a point of covalent attachment to an NRPS carrier protein domain, nor is it a macrocyclized product, as the thiotemplated model of nonribosomal peptide synthesis dictates (15). Vibriobactin is instead a triacylated triamine, which necessitates intermediates on route to the finished product to be free, soluble molecules instead of phosphopantetheine-tethered thioesters of a typical NRPS.

Vibriobactin synthetase, along with its receptor, transporter, and utilization genes, is split between two gene clusters located approximately 1 megabase apart (16) on replicon I of the *V. cholerae* chromosome (12, 13, 17). In the companion paper (18), we characterized VibB, VibE, and VibH, the three biosynthetic proteins of the first gene cluster, culminating in the *in vitro* synthesis of *N*¹-(2,3-dihydroxybenzoyl)norspermidine (7). This product possesses one of the three acylations required for vibriobactin. Herein, we focus on the second gene cluster, which contains the megasynthetase VibF (12), a 270 kDa, 2413-residue, six-domain protein. We have heterologously expressed and purified this multidomain enzyme, and for the first time, we demonstrate enzymatic oxazoline formation from cyclization/dehydration of threonine by an NRPS. Furthermore, we show that the VibH product 7 is acylated twice by VibF on its two remaining free amines by VibF-bound 2-(2,3-dihydroxyphenyl)-5-methyloxazoline-4-carboxylates to form vibriobactin. These acylations are novel activities for an NRPS as they represent condensation and amide bond formations between an upstream, carrier-protein-bound donor and a downstream, soluble amine acceptor. We propose that two unusual condensation (C) domains embedded in VibF are responsible for these activities.

EXPERIMENTAL PROCEDURES

Materials and Methods. For general procedures and reagents, see the accompanying paper (18).

Cloning and Sequencing of *vibF*. VibF was amplified by PCR from *V. cholerae* O395 genomic DNA in two pieces by use of the following primer pairs (VibF1F, 5'-GGGTT-TACATATGAAAGAAATGACCGCAATGCAAG-3', and VibF1R, 5'-CAACGGTTCGAC CATAACGGGATCAGCT-GACATCATC-3'; and VibF2F, 5'-CATATGGTCGAC-CGTTGGCGGGAAACCGTTATTTC-3', and VibF2R, 5'-ACAAAAC**CTCGAG**CCCCATGGACGGAGAGCGACAA-3'); restriction sites are underlined, and mutations are shown in boldface type. The two amplicons were digested with restriction endonucleases *Nde*I and *Sal*I and with *Sal*I and *Xho*I, respectively, and then ligated sequentially to the corresponding sites of pET37b (Novagen). The resulting plasmid, pVibF, expresses a translational fusion of VibF with a C-terminal octahistidine affinity tag. This plasmid was used to transform *E. coli* DH5 α , and then transferred to strain BL21(DE3) for expression after DNA sequencing to verify the fidelity of the PCR amplifications.

Expression and Purification of VibF and Accessory Proteins. VibF was expressed and purified from *E. coli* BL21(DE3) containing the plasmid pVibF. Culture (3 \times 1 L) in Luria-Bertani broth supplemented with kanamycin (50 μ g/mL) and 2 mM MgCl₂ was grown for 36 h at 250 rpm, 20 °C, with expression from the T7 promoter allowed to induce naturally during stationary phase. Harvested cells were lysed by French press into 20 mM Tris, pH 8.0, 500 mM NaCl, and 1 mM MgCl₂, the lysate was clarified by ultracentrifugation, and the supernatant was incubated with 2 mL of Qiagen Ni-NTA Superflow resin overnight. VibF was eluted with a linear gradient of imidazole from 20 to 100 mM over 20 column volumes and then analyzed by SDS-PAGE. Fractions containing pure protein were pooled and dialyzed against 20 mM Tris, pH 8.0, 50 mM NaCl, 1 mM DTT, and 10% glycerol. Samples were quantified by absorbance at 280 nm with the predicted molar extinction coefficient (ϵ = 294 290 M⁻¹ cm⁻¹), and by the Bradford protein dye assay (Bio-Rad). Samples were aliquotted and stored frozen at -80 °C until use.

VibE, VibB, and VibH were expressed and purified as described (18).

Phosphopantetheinylation of VibF. Prior to use in acylation assays, VibF was modified with phosphopantetheine in the following manner. Reactions (100 μ L) contained 75 mM Tris, pH 7.5, 10 mM MgCl₂, 2 mM TCEP, 1 μ M VibF, 0.1 mM coenzyme A, and 0.3 μ M Sfp and were incubated for 60 min at 30 °C.

ATP-PP_i Exchange Assay for VibF Substrate Specificity. Substrate-dependent ATP-PP_i exchange assays (100 μ L) containing 10–100 nM VibF were performed as described (18).

Analysis of Covalent Self-Thioesterification of Holo-VibF. Acylation of VibF with radiolabeled amino acids was assayed as follows. Reactions (25 μ L) contained 75 mM Tris, pH 7.5, 10 mM MgCl₂, 0.5 M NaCl, 5 mM TCEP, 5 mM ATP, 2 μ M holo-VibF, and either 43 μ M [¹⁴C]-L-Thr (0.2 μ Ci), 1.56 mM [¹⁴C]-2-aminobutyrate (0.35 μ Ci), or 0.5 mM [³H]-L-Ser (1.2 μ Ci). Reactions were incubated at 30 °C for various lengths of time and worked up as described (18).

Large-Scale Preparation of DHB-NSPD and DHB-DAH. For DHB-NSPD, a 5 mL reaction contained 75 mM Tris, pH 7.5, 10 mM MgCl₂, 1 mM TCEP, 50 μ M CoASH, 4 mM DHB, 4 mM NSPD, 120 nM Sfp, 5 mM ATP, 5 μ M VibB, 1 μ M VibE, and 1 μ M VibH. Half the total amount of VibE and VibH was added to initiate, followed by the remaining amount after 1 h. After a total incubation of 3 h at 30 °C, 45 mL of cold methanol was added, followed by removal of precipitated material by centrifugation. The solvent was removed under vacuum, and DHB-NSPD was purified by preparative reverse-phase HPLC. For DHB-DAH, a 5 mL reaction contained identical components except for the addition of 6 mM DHB, 7 mM DAH, 10 mM ATP, and 2 μ M VibB.

Formation of DHP-Oxazoline and Transfer to Various Nucleophilic Amines. Reactions (100 μ L) contained 75 mM Tris, pH 7.5, 10 mM MgCl₂, 2 mM TCEP, 200 μ M 2,3-DHB, 10 mM L-Thr, 5 mM ATP, 5 μ M VibB, 1 μ M VibE, either 0.2 or 1 μ M VibF, and various amounts of acceptor amine. Reactions were incubated at 30 °C for a time predetermined to give a steady-state rate. Reactions were quenched by the addition of 900 μ L of cold methanol and precipitate removed by centrifugation for 30 min at 4 °C. Products were dried under vacuum, redissolved in 30% acetonitrile, and analyzed by HPLC as described previously. For MALDI-TOF mass spectrometric and ¹H NMR analysis of reaction products, large-scale enzymatic reactions as above were purified by preparative HPLC and lyophilized in the dark. Analyses were performed as described previously. HPLC product peak areas were converted to nanomoles of product by use of a standard curve constructed with purified **6** (for compounds **5** and **6**) or by calculation of the conversion factor from standard curves for **6** and **7** (for compounds **2–4**).

Large-Scale Preparation of **6 by VibF.** A 2.4 mL reaction containing 75 mM Tris, pH 7.5, 10 mM MgCl₂, 1 mM TCEP, 50 μ M CoASH, 4 mM DHB, 10 mM L-Thr, 2 mM NSPD, 220 nM Sfp, 10 mM ATP, 5 μ M VibB, 1 μ M VibE, 100 nM VibH, and 1 μ M VibF was incubated for 6 h at 30 °C before workup and purification as above for DHB-NSPD.

Formation of Vibriobactin from **6 by VibF.** Reactions (200 μ L) contained 75 mM Tris, pH 7.5, 10 mM MgCl₂, 2 mM TCEP, 1 mM CoASH, 200 μ M DHB, 10 mM L-Thr, 5 mM ATP, 5 μ M VibB, 500 nM VibE, 50 nM VibF, 300 nM Sfp, and 0–400 μ M **6**. After initiation with ATP, reactions proceeded for 4 min at 30 °C before cold methanol quench, workup, and analysis as above. HPLC product peak areas were converted to nanomoles of vibriobactin by calculation of the conversion factor from standard curves for **6** and **7**.

Formation of Vibriobactin by VibB, VibH, VibE, and VibF. Reactions (100 μ L) contained 75 mM Tris, pH 7.5, 10 mM MgCl₂, 2 mM TCEP, 1 mM CoASH, 400 μ M DHB, 10 mM L-Thr, 2.5 mM NSPD, 5 mM ATP, 5 μ M VibB, 2 μ M VibE, 500 nM VibF, 300 nM Sfp, and 0–100 nM VibH. Each reaction was initiated with ATP and stopped at 0–20 min time points with cold methanol as above.

RESULTS

Cloning and Sequencing of *vibF*. The 7239 bp gene *vibF* was amplified from chromosomal DNA and cloned in two pieces to facilitate both the PCR and sequencing. The PCR primers introduce a silent N-terminal mutation to optimize

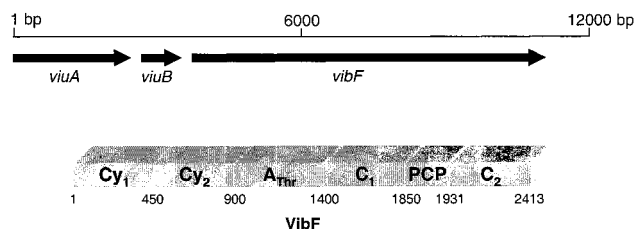


FIGURE 2: Second gene cluster of vibriobactin synthetase (12) [for the first gene cluster, containing *vibB*, *vibE*, and *vibH*, see the accompanying paper (18)]. *ViuA* is the vibriobactin outer membrane receptor (30). *ViuB* is a cytoplasmic protein necessary for ferric vibriobactin utilization (31). *VibF* is a nonribosomal peptide synthetase and one of four proteins required for vibriobactin biosynthesis. Domain analysis of *VibF* yields six domains: Cy = cyclization; A_{Thr} = adenylation, specific for threonine; C = condensation; PCP = peptidyl carrier protein. Amino acid residues marking predicted domain boundaries are listed below the *VibF* schematic.

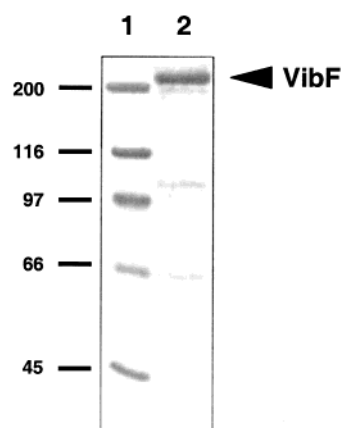


FIGURE 3: Coomassie-blue stained 9% SDS-PAGE gel of purified *VibF* (2413 residues, 270 kDa). Lane 1, molecular weight standards; lane 2, *VibF* purified by His-tagged nickel affinity chromatography.

codon usage in *E. coli*, as well as silent mutations that destroy an internal *NdeI* site and introduce an adjacent *SalI* site. The overexpression plasmid, p*VibF*, appends the sequence LEHHHHHHHH to *VibF*; this octahistidine tag has been successful in the affinity purification of very large NRPS proteins previously (19). In sequencing p*VibF*, seven non-primer-introduced nucleotide changes were found, as compared to the partial *vibF* sequence in GenBank (accession number AF030977) (12). Of these, two were silent, while the remaining five matched the nucleotide sequence of *vibF* from *V. cholerae* serotype O1 as sequenced by TIGR (20). This revised sequence for complete *vibF* has been deposited in GenBank (accession number AF287255).

Expression and Purification of *VibF*. Expression of the six-domain, 270 kDa protein *VibF* (Figure 2) from *E. coli* strain BL21(DE3) was most successful when cultures were allowed to incubate for 36 h at 20 °C without induction. Higher growth temperatures or IPTG induction resulted in larger amounts of insoluble protein. Single-step nickel-affinity chromatography of the clarified cellular lysates resulted in pure *VibF* with a yield of 0.5 mg/L of culture. SDS-PAGE of the purified *VibF* is shown in Figure 3.

Covalent Phosphopantetheinylation of *VibF*. Sequence analysis of *VibF* identified a PCP domain located between residues 1850 and 1931 (Figure 2). We attempted phosphopantetheinylation of this domain using the PPTase Sfp and

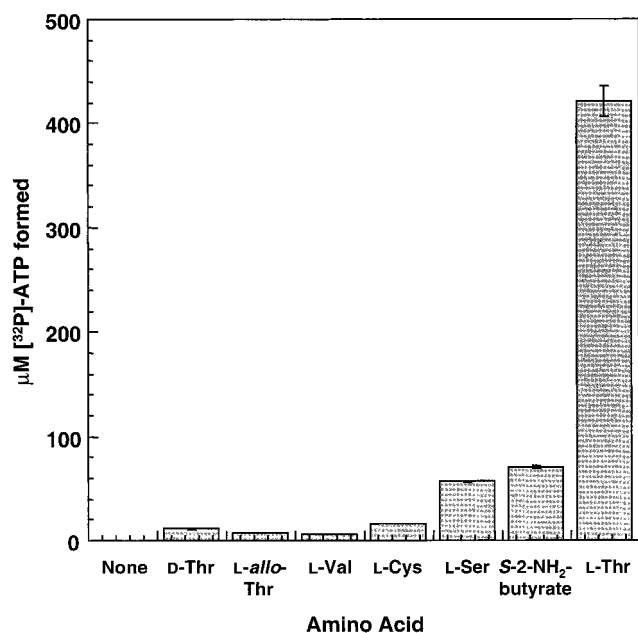


FIGURE 4: Adenylation specificity profile of the VibF A domain. The incorporation of [32 P]PP $_i$ into ATP was measured by the ATP–PP $_i$ exchange assay as described under Experimental Procedures. The bars indicate micromoles of label per liter exchanged by 50 nM VibF in 45 min with 10 mM of the indicated amino acid present.

Table 1: Kinetics of ATP–PP $_i$ Exchange Catalyzed by VibF

substrate	k_{cat} (min $^{-1}$)	K_m (mM)	k_{cat}/K_m (s $^{-1}$ M $^{-1}$)
L-threonine	920 \pm 14	2.2 \pm 0.1	7.0 \times 10 3
S-2-aminobutyrate	80 \pm 1	6.9 \pm 0.4	1.9 \times 10 2
L-serine	260 \pm 9	43 \pm 3	1.0 \times 10 2

CoA. When initial experiments showed little incorporation of [3 H] label from tritiated CoA, we measured the stoichiometric levels of [14 C]-L-threonine incorporation into VibF with and without Sfp phosphopantetheinylation. Unmodified VibF could be labeled to 46% stoichiometry with L-Thr, and Sfp/CoA treatment increased this level to 53%. This indicates that most of VibF is converted to the holo form by *E. coli* PPTases in vivo during the long growth and induction period.

ATP–PP $_i$ Exchange Assay for VibF Substrate Specificity. Sequence analysis of VibF identified an adenylation (A) domain located between residues 900 and 1400 (Figure 2). Results for the substrate-dependent ATP–PP $_i$ exchange reaction catalyzed by VibF are shown in Figure 4 and Table 1. Along with the presumed natural substrate L-threonine, we tested D-Thr, L-allo-Thr, L-Val, L-Cys, L-Ser, and (S)-2-aminobutyrate. While several of these substrates gave weak signals above background in the exchange assay (Figure 4), only L-Thr, L-Ser, and (S)-2-aminobutyrate were deemed sufficiently active to measure kinetic constants, shown in Table 1.

Analysis of Covalent Self-Thioesterification of Holo-VibF. To verify the transfer of aminoacyl adenylate from the A domain to the holo-PCP thiol, radiolabeled L-Thr, L-Ser, and 2-aminobutyrate were incubated for varying lengths of time with holo-VibF and ATP, and radiolabeled VibF was detected by TCA precipitation and scintillation counting. At amino acid concentrations well below their K_m for ATP–PP $_i$ exchange, L-Thr and 2-aminobutyrate reached their final stoichiometries of 25% and 65% after 5 and 7.5 min,

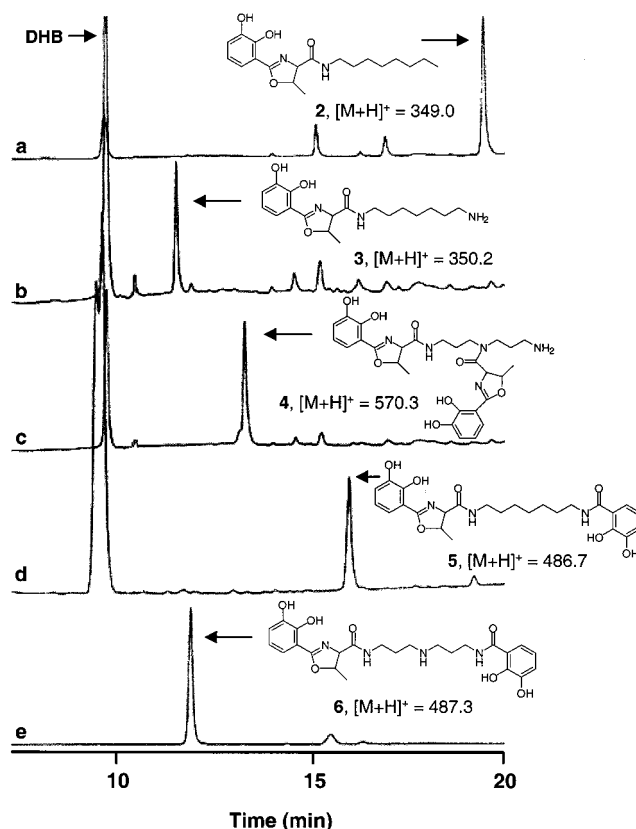


FIGURE 5: HPLC elution profiles of oxazoline-containing amides formed by VibF. Reactions contained VibE, VibB, VibF, DHB, L-Thr, ATP, and one of the following amines: (a) octylamine, (b) 1,7-diaminoheptane, (c) norspermidine, (d) DHB-diaminoheptane, or (e) DHB-norspermidine as amine acceptor substrates. Reaction products are indicated with arrows, and the masses obtained by MALDI-TOF analysis are listed. The small peak at 15.3 min of trace e is vibriobactin (see Figures 9 and 10).

respectively. L-Ser was not transferred efficiently and achieved only 15% stoichiometry after 1 h.

Large-Scale Preparation of DHB-NSPD and DHB-DAH. To prepare enough DHB-NSPD (**7**) and DHB-DAH for testing as substrates for VibF, large-scale enzymatic reactions were performed with VibB, VibE, VibH, DHB, and NSPD or DAH. After preparative HPLC purification, 5 mL reactions yielded 6.5 and 5.2 mg of **7** and DHB-DAH, respectively. These compounds were dissolved in 75 mM Tris, pH 7.5, to a stock concentration of 100 mM.

Acylation of Primary Amines with DHP-Oxazolinecarboxylate by VibF. With threonylation of holo-VibF established, we looked for formation and turnover of DHP-oxazolinecarboxylate resulting from hydrolysis of the expected product of VibE, VibB, DHB, and L-Thr with VibF (Figure 6). When this system failed to turn over catalytically (data not shown), we attempted addition of various amines to facilitate catalytic release of the postulated DHP-oxazolinecarboxylate species. HPLC traces of these assays are shown in Figure 5. Major product peaks appeared with the addition of octylamine, 1,7-diaminoheptane, norspermidine, **7**, and DHB-DAH. All products were ATP-, amine-, and threonine-dependent. The mass of each of these new products was determined by mass spectrometric analysis (listed with the structures in Figure 5) and was consistent with the calculated mass. Four of the products were monoacylated with DHP-oxazolinecarboxylate, while one, bis(DHP-ox-

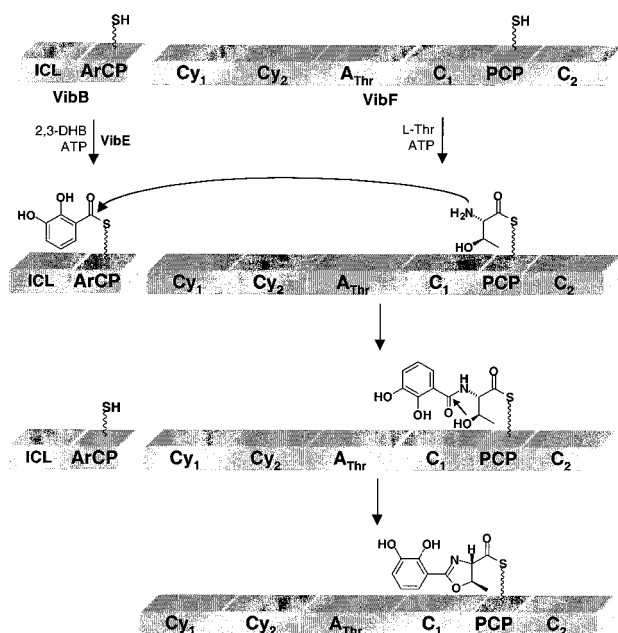


FIGURE 6: 2-(2,3-Dihydroxyphenyl)oxazoline formation by VibB and VibF. In the first, loading step, holo-VibB is acylated with DHB by VibE [VibB is a bifunctional protein, ICL = isochorismate lyase; see accompanying paper (18)], while VibF self-aminoacylates its PCP domain with its A domain. VibF then condenses, heterocyclizes, and dehydrates the two substrates, presumably mediated by one of the two Cy domains. (Although the amide bond is drawn being formed first, this has not been established.) Finally, the 2-(2,3-dihydroxyphenyl)-5-methyloxazoline-acyl enzyme thioester is then ready for condensation with an amine, which is presumably catalyzed by one or both of the C domains.

azolinecarbonyl)norspermidine (**4**), was bisacylated. The absence of identifiable monoacylated (DHP-oxazolinecarbonyl)norspermidine indicates that the second transfer of DHP-oxazoline is rapid compared to the first. The regiochemistry of the two acylations on **4** was not determined.

Products **5** and **6** represent VibF transfers of DHP-oxazoline to amines monoacylated with DHB by the VibH enzyme. The latter structure possesses two of the three acylations of mature vibriobactin. The regiochemistry of acylation for **6** was confirmed by ^1H NMR spectroscopy: the symmetry present in the norspermidine methylene resonances supports acylation of both primary amines, rather than one primary and the secondary. In addition, because the $J_{\alpha\beta} = 7.2$ Hz, the stereochemistry of the oxazoline ring is assigned as *trans* ($J_{\text{cis}} > 10$ Hz). Compound **6** (200 MHz, CD_3OD): δ 7.18 (m, 2H), 6.95 (m, 2H), 6.72 (m, 2H), 4.48 (d, 1H, $J = 7.2$ Hz), 3.51 (t, 2H, $J = 6.6$ Hz), 3.39 (m, 2H), 3.04 (m, 4H), 1.95 (m, 4H), and 1.53 (d, 1H, $J = 6.2$ Hz); the oxazoline β -H was obliterated by the solvent signal.

Kinetics of DHP-Oxazolinecarboxylate Acylation of Primary Amines by VibF. For the five successful amine substrates, apparent kinetic constants measured from formation of products **2–6** by VibF are listed in Table 2. Condensation of DHP-oxazolinecarboxylate with unacylated substrates octylamine, 1,7-diaminoheptane, and norspermidine all yielded k_{cat} values in the 1–5 min^{-1} range, with the K_m for norspermidine (5.8 mM) 2.5-fold higher than that for octylamine (2.2 mM), and 4.3-fold lower than for 1,7-diaminoheptane (25 mM).

The apparent kinetic data for the two DHB-capped substrates DHB-DAH and DHB-NSPD were far superior

Table 2: Kinetics of DHP-Oxazoline Transfer to Primary Amines by VibF

substrate	k_{cat} (min^{-1})	K_m (μM)	k_{cat}/K_m ($\text{s}^{-1} \text{M}^{-1}$)
octylamine	5.4 ± 0.4	2200 ± 300	41
1,7-diaminoheptane	1.5 ± 0.1	25000 ± 3000	1.0
norspermidine	1.3 ± 0.1	5800 ± 1500	3.7
DHB-diaminoheptane	20.5 ± 0.1	36 ± 1	9490
DHB-norspermidine	122 ± 5	1.7 ± 0.4	1.2×10^6

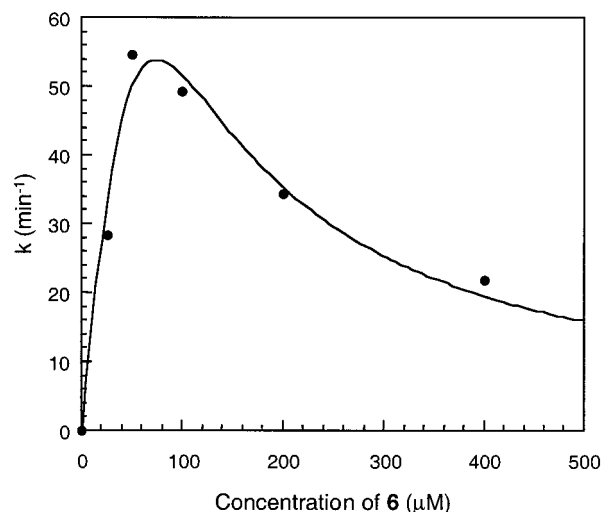


FIGURE 7: Kinetics of DHP-oxazolinecarboxylate transfer to the secondary amine of **6** by VibF to form vibriobactin (see also Figure 8). Reactions contained VibE, VibB, VibF, DHB, L-Thr, ATP and increasing concentrations of **6**. The plotted points were fit to the general substrate inhibition equation. The maximum k was observed at 50 μM **6**: 55 min^{-1} .

(Table 2, Figure 8). VibF acylated DHB-DAH with DHP-oxazolinecarboxylate to form **5** with a k_{cat} of 20.5 min^{-1} and $K_m = 36 \mu\text{M}$, while DHB-NSPD was acylated to **6** with $k_{\text{cat}} = 122 \text{ min}^{-1}$ and a low K_m of 1.7 μM . This last substrate was thus 130-fold better than DHB-DAH in catalytic efficiency, 30000-fold better than octylamine, and (3.2×10^5) -fold better than norspermidine. The importance of the central, secondary amine of NSPD in recognition and catalysis is apparent in the 130-fold increase in the efficiency of use of DHB-NSPD as compared to DHB-DAH.

Large-Scale Preparation of 6. To prepare enough **6** for testing as a substrate for VibF, a large-scale enzymatic reaction was performed with VibB, VibE, VibH, VibF, DHB, L-Thr, and NSPD. After preparative HPLC purification, a 2.4 mL reaction yielded 2.0 mg of **6**. This compound was dissolved in 75 mM Tris, pH 7.5, to a stock concentration of 50 mM.

Analysis of Vibriobactin Production from 6 by VibF. When the diacylated substrate **6** was reintroduced as substrate with VibB, VibE, VibF, DHB, L-Thr, and ATP, a single new product peak was formed, eluting at 15.3 min in our HPLC gradient (Figure 9). This product was collected, and mass spectrometry provided a mass consistent with vibriobactin ($[\text{M} + \text{H}]^+ m/z$ calcd 706.27, found 706.10). Chemically, this represents acylation of the central, secondary amine of **6** with DHP-oxazolinecarboxylate (Figure 8). The ultraviolet spectrum of this product was also consistent with data published previously for natural vibriobactin ($\text{UV}_{\text{max}} = 258, 318 \text{ nm}$; ratio = 4:1). Finally, 1.6 mg of this product was

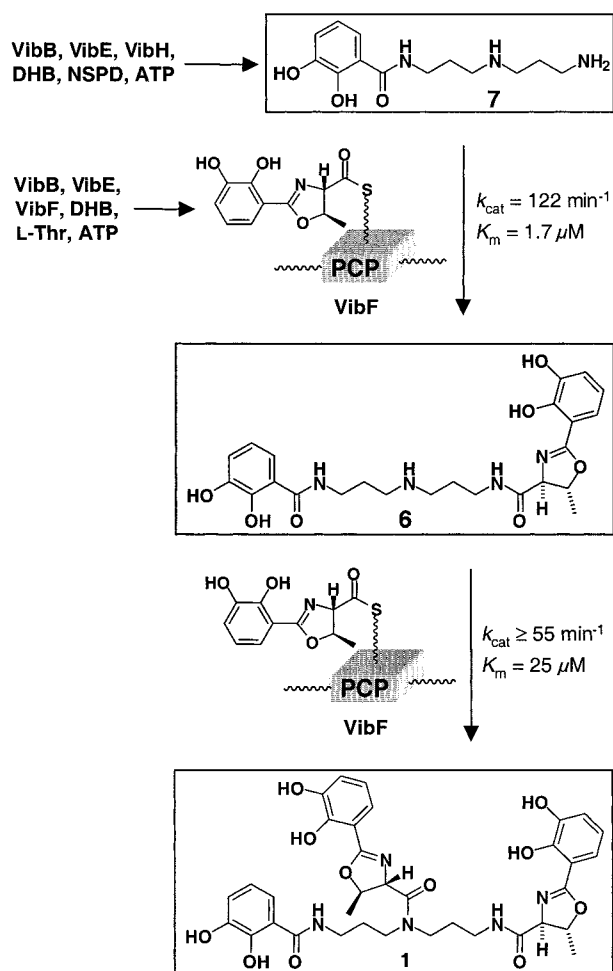


FIGURE 8: Completion of vibriobactin biosynthesis from DHB-NSPD (7) by VibF. NSPD is acylated with DHB-(S)-VibB by VibH, producing 7 [see accompanying paper (18)]. DHB-NSPD is then acylated by DHP-oxazolinecarbonyl-(S)-VibF on its primary amine to yield 6, which then undergoes a second acylation with the identical VibF-derived donor, but this time on the remaining secondary amine, to produce vibriobactin (1). Apparent kinetic constants for the final two acylation steps are listed. We propose that the two DHP-oxazoline acylations of 7 and 6 are catalyzed by the C₁ and C₂ domains of VibF, although the domain responsible for each step has not yet been determined.

produced enzymatically and the ¹H NMR spectrum was matched to that published for natural vibriobactin. ¹H NMR (200 MHz, CD₃OD): δ 7.22–6.65 (m, 9H), 5.30 (dt, 1H, $J = 16.2$ and 5.8 Hz), 5.07–4.90 (m, 1H), 4.73 (d, 1H, $J = 2.2$ Hz), 4.49 (d, 1H, $J = 7.4$ Hz), 3.66–3.20 (m, 8H), 2.01 (m, 2H), 1.87 (dt, 2H, $J = 7.0$ and 7.0 Hz), 1.57 (d, 0.5H, $J = 6.0$ Hz), 1.54 (d, 0.5H, $J = 5.8$ Hz), 1.45 (d, 0.5H, $J = 6.6$ Hz), and 1.29 (d, 0.5H, $J = 5.2$ Hz). Amide rotational isomers are apparent in the doubled signals for the oxazoline β - and γ -protons.

Kinetics of vibriobactin formation by VibF from intermediate 6 as substrate are plotted in Figure 7. Substantial substrate inhibition was observed at substrate concentrations above $50 \mu\text{M}$, preventing the determination of Michaelis–Menten constants. The maximum k observed for this step was 55 min^{-1} , with half this velocity reached at $25 \mu\text{M}$ substrate (K_m) (Figure 8).

Time Course of Vibriobactin Biosynthesis by VibBEFH. When the four proteins VibE, holo-VibB, VibH, and holo-

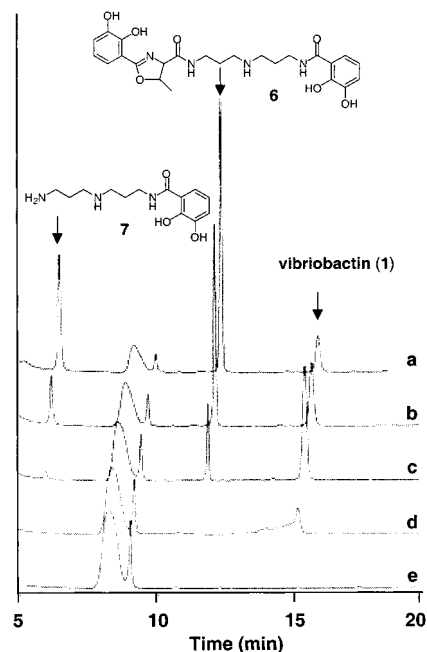


FIGURE 9: HPLC elution profiles of vibriobactin-forming reactions containing various amounts of VibH, demonstrating the sensitivity of relative accumulation of intermediates 7 and 6 and vibriobactin to the concentration of VibH, the condensation enzyme that forms the first soluble intermediate 7. All reactions represent the 5 min time point of the time courses presented in Figure 10. Reactions contained VibE, VibB, VibF, DHB, NSPD, and ATP, plus VibH to a final concentration of (a) 100, (b) 50, (c) 20, (d) 10, and (e) 0 nM. Plots have a x-coordinate offset of 0.25 min; the broad peaks at 8–9 min are unreacted DHB.

VibF were combined with DHB, L-Thr, NSPD, and ATP, three products, identified as DHB-NSPD, DHP-oxazolinyl-NSPD-DHB, and vibriobactin, were detected. By varying the concentration of VibH while the other protein and substrate concentrations were fixed, the relative amounts of these three products could be manipulated. HPLC traces of the 5 min point of five reactions containing different VibH concentrations are shown in Figure 9. The complete time courses for reactions containing 10, 20, 50, and 100 nM VibH are shown in Figure 10. At 0 nM VibH, no products are seen. At 10 nM VibH, only vibriobactin, and not the two intermediates, are observed, with vibriobactin produced at a linear rate of $15 \mu\text{M}/\text{min}$. At 20 nM VibH, vibriobactin is still the major product ($20 \mu\text{M}/\text{min}$), but intermediates 6 and 7 accumulate at rates of $10 \mu\text{M}/\text{min}$ and $2 \mu\text{M}/\text{min}$, respectively. At higher concentrations of VibH, this trend accelerates so that 6 and 7 become the major products, while vibriobactin production falls off to $10 \mu\text{M}/\text{min}$ and $5 \mu\text{M}/\text{min}$ at 50 and 100 nM VibH, respectively.

DISCUSSION

The genes that encode the machinery for biosynthesis of the *V. cholerae* iron chelator vibriobactin are split between two gene clusters separated by 1 megabase on the larger of the bacterium's two chromosomes (16). Characterization of three of the four required proteins, the 2,3-DHB–AMP ligase VibE, the bifunctional isochorismate lyase–aryl carrier protein VibB, and the amide synthase VibH, was described in the accompanying paper (18) and culminated in the biosynthesis of DHB-NSPD (7). The fourth protein is the

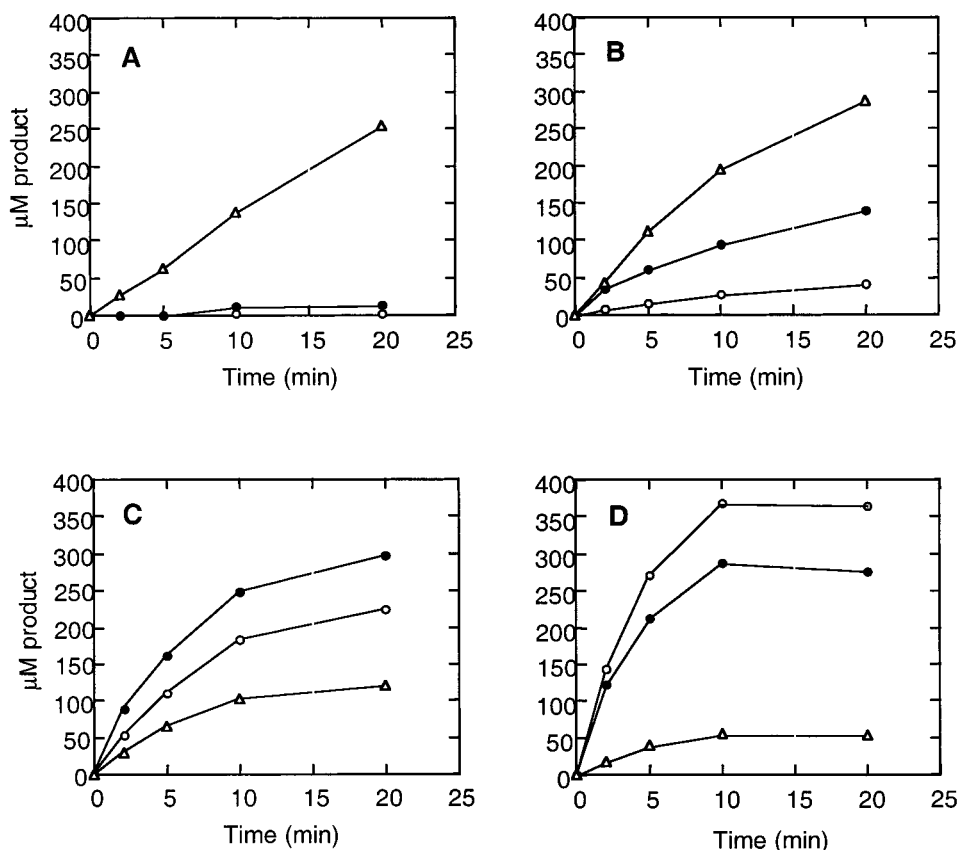


FIGURE 10: Effect of varying the concentration of VibH on vibriobactin production. Plots represent time courses of production of vibriobactin (Δ), **6** (\bullet), and **7** (\circ) by 5 μ M VibB, 2 μ M VibE, and 500 nM VibF in the presence of (A) 10, (B) 20, (C) 50, or (D) 100 nM VibH. In the absence of VibH, no products were observed under these conditions (Figure 9e).

recently identified VibF, located in the second gene cluster (12). Originally cloned as a 2158 residue, C-terminal-truncated fragment, VibF was assigned to the family of nonribosomal peptide synthetases on the basis of sequence homology that identified an adenylation (A) domain, a peptidyl carrier protein (PCP) domain, and a condensation (C) domain (12). By using this published clone to search preliminary *V. cholerae* sequence data from The Institute for Genomic Research (TIGR), we identified a complete *vibF* open reading frame that encodes a 2413 residue protein (Figure 2). Sequence analysis of *vibF* allowed the predictive assignment of six functional domains in an unusual arrangement (Figure 2): unique tandem cyclization–cyclization domains (Cy–Cy), followed by the A domain, then a domain with weak homology to C domains (C_1), followed by the PCP domain, and terminating in another C domain (C_2). The conserved core motifs for Cy₁, Cy₂, A, and PCP were readily identified, although of the seven conserved residues shared by Cy and C domains identified by Konz et al. (21), all seven were found in Cy₁, while three were changed in Cy₂ (I506 for expected H, F694 for T, and E734 for F). For C_2 , the key catalytic core C3 (HHxxxDGWS) was present as HHIVLDEWS, and cores C1, C2, C4, C5, and C6 (but not C7) could be found. In contrast, the domain assigned as C_1 was much more poorly conserved, with C3 present as HQIIEQWD, with C1, C2, and C4 only weakly represented, and with C5–C7 missing entirely. The second His and the Asp of core C3 have been shown by mutation to be required for NRPS condensation function (22); these residues are replaced by Gln and Glu in C_1 . The length of C_1 , however,

at 450 residues, matches the accepted value for C domains (22).

Remarkably, heterologous expression of this very large polypeptide (270 kDa) was successful in *E. coli* under low-temperature growth conditions without induction. Subsequent affinity purification yielded usable quantities of VibF (Figure 3). The long expression time appears to result in the production of mostly holoprotein, as Sfp and CoA were able to only marginally increase levels of phosphopantetheinylation at Ser1891, as judged by covalent acylation with L-Thr.

The A domain of VibF was assayed both for amino acid activation and for transfer of activated substrate to the holo-PCP domain. The ATP–PP_i exchange assay demonstrated clear selectivity for L-Thr, the amino acid present in vibriobactin (Figure 4 and Table 1) (1). Stereoisomers D-Thr and L-*allo*-Thr were activated very poorly, as was the isosteric substrate L-Val. Smaller amino acids with similar side-chain moieties [in this case, L-Cys, L-Ser, and (S)-2-aminobutyrate] generally present difficulties for aminoacyl-tRNA synthetases (AARS) (23) and are discriminated against here less well than the isosteric substrates: the unnatural amino acid (S)-2-aminobutyrate is down 37-fold in catalytic efficiency, and L-Ser is down 70-fold. For comparison, ThrRS discriminates against L-Ser by 1000-fold versus L-Thr (23).

In the second step of A domain activity, the aminoacyl-AMP substrate is thioesterified to the phosphopantetheinyl arm of holo-PCP. VibF was able to aminoacylate itself with the three radiolabeled substrates L-Thr, 2-aminobutyrate, and L-Ser, although L-Ser transferred very poorly. The final

stoichiometries (25% for L-Thr, 65% for 2-aminobutyrate, 15% for L-Ser) did not reach 100%, and these values are difficult to rationalize. This behavior has been observed previously in other NRPS systems (9, 19, 24), and may reflect incomplete phosphopantetheinylation, incorrect specific radioactivity of the substrates, different equilibrium constants of transfer for different substrates, or actual substoichiometric acylation. We conclude, however, that covalent aminoacylation occurs, and the subsequent results bear out robust overall activity for VibF.

According to precedent from the thiazoline-forming yersiniabactin and pyochelin synthetases (9, 25), oxazoline formation by VibF should proceed from DHB-loaded VibB and Thr-loaded VibF, catalyzed by a Cy domain. This mechanism is shown in Figure 6. Oxazoline biosynthesis requires initial bond condensation (drawn, but not established, as the amide bond) and is followed by heterocyclization and dehydration to the 2-(2,3-dihydroxyphenyl)-5-methyloxazoline-acyl-enzyme species, all presumably catalyzed by Cy₁ or Cy₂. However, we were unable to detect turnover of a coupled and cyclized DHP-oxazolinecarboxylate substrate by HPLC. This is likely because this species remains thioesterified to the PCP of VibF and is not readily hydrolyzed and released into solution (Figure 6). To provoke release and turnover of this aryl oxazoline, exogenous primary amines were added to the reaction mixture. VibF condensed the inferred DHP-oxazoline-acyl-enzyme intermediate with five of these substrates, yielding the oxazoline-containing products 2–6 identified in Figure 5 with mass spectral data. Although Cy-domain-mediated thiazoline formation from cysteine has been shown (9, 25), and one other oxazoline-specific Cy domain has been identified, but not assayed (26), this represents the first demonstration of oxazoline formation by an NRPS Cy domain. Which of the two tandem Cy domains catalyzes this step remains as yet undetermined.

The fact that diaminoheptane was acylated only once, despite its two free amines, demonstrated clear discrimination against a second primary amine acylation step. Norspermidine on the other hand was exclusively acylated twice, and while the regiochemistry of 4 could not be determined, the circumstantial evidence of monoacylation product 3 as well as the structure of vibriobactin point to acylation of one primary and the secondary amine. Exclusive detection of the bisacylated product 4 was likely due to rapid second transfer to the monoacylated intermediate. VibF possesses two C domains (Figure 2), and it is unknown which of these catalyzes acyl transfer to the free amine. Furthermore, it is not clear at present whether the same C domain catalyzes transfer to both primary and secondary amines, or if these activities are distinct.

For the three uncapped substrates (octylamine, diaminoheptane, and norspermidine), kinetics of transfer are relatively poor (Table 2). For the two DHB-acylated substrates, the kinetics of transfer of DHP-oxazolinecarboxylate from VibF are dramatically improved. DHB-NSPD (7) is acylated some (3×10^5)-fold more efficiently than uncapped norspermidine, while DHB-DAH was 10^4 better than DAH. Product 6 is acylated exclusively on the primary amine, as determined by the NMR spectrum. The desamino substrate DHB-DAH is down 120-fold in catalytic efficiency relative to the presumed natural substrate 7, showing that although the

central amine is not acylated in this step, its presence is important for efficient binding and acylation of the primary amine.

The end product vibriobactin is also detected in reactions with intermediates 7 or with 6 introduced as substrates for VibF and results from either bisacylation (to 7) or monoacylation (to 6) with DHP-oxazoline. To isolate this latter VibF acylation step for kinetic measurement, 6 was purified from enzymatic reactions and used as substrate for the production of vibriobactin (Figures 7 and 8). Severe substrate inhibition of the acylation reaction prevented measurement of Michaelis–Menten kinetics, but the formation of vibriobactin was robust.

If NSPD is incubated with VibB, VibE, VibF, VibH, and sufficient DHB, L-Thr, and ATP, vibriobactin is produced (Figures 8 and 9), thus reconstituting the entire synthetase. Vibriobactin arises from three sequential acylations of norspermidine: first, primary amine capping with VibB-derived DHB, catalyzed by VibH (18); second, primary amine capping with the DHP-oxazoline-acyl moiety from the PCP of VibF, catalyzed by VibF, and finally, acylation of the secondary amine, again with the DHP-oxazoline-acyl group by VibF (Figure 8). The combination of three separate acylation reactions catalyzed by two enzymes with evidence of some degree of substrate inhibition in the first and third cappings predicts that flux through the system may have a complex dependence on enzyme and substrate concentrations, particularly the diffusible intermediates 6 and 7. To test this, we titrated VibH at fixed VibF and NSPD concentrations (Figures 9 and 10). As VibH concentration is increased, the rate of vibriobactin formation increases, then peaks, and ultimately drops. Meanwhile the intermediates 7 and 6, which do not accumulate at low VibH, become the major products at high VibH. Due to the high catalytic efficiency of the first two acylations, this occurs as 6 reaches inhibitory concentrations ($\sim 100 \mu\text{M}$), which causes a drastic slowing in the rate of the third acylation to vibriobactin, and thus even more accumulation of 6. Low concentrations of VibH slow the rate of 7, and thus 6 formation, allowing the final acylation to escape substrate inhibition. This all points to vibriobactin synthetase being a system very sensitive to relative and absolute enzyme, substrate, and intermediate concentrations and one that is likely balanced to most efficiently take advantage of cellular concentrations of substrates to produce vibriobactin without leaving partially formed products to accumulate.

Vibriobactin biosynthesis presents a different picture from the NRPS paradigm of linear, stepwise chain elongation of stoichiometric, carrier-protein-bound substrates and intermediates (14). Rather than being a linear or cyclized peptide whose final structure is evident from the domain organization of its synthetase proteins, vibriobactin is a triacylated triamine, lacking a carboxylate in the norspermidine backbone that would allow thioesterification and immobilization of a linearly growing chain. Vibriobactin synthetase uses the enzymatic domains of an NRPS to produce the two different acyl caps for vibriobactin: DHB and 2-DHP-5-methyloxazoline-4-carboxylate (Figure 6); the latter is employed twice to yield the bis-DHP-oxazolines of 1. These carrier-protein-attached species are then transferred sequentially to the three amines of norspermidine by three specialized C domains. These C domains (VibH and C₁ and C₂ of VibF) share

homology with standard C domains but bind an upstream carrier protein thioester and a downstream soluble amine and are chemically more analogous to aminotransferase enzymes such as *N*-myristoyltransferase (myristoyl-CoA to *N*-terminal glycines) (27) and aminoglycoside 3-*N*-acetyltransferase (acetyl-CoA to aminoglycoside antibiotics) (28). Because the acceptor amine for each of the C domains is a soluble molecule, there is no need for a C-terminal thioesterase domain to release the final product; after the third acylation (of the secondary amine), VibF turns over the product into solution.

Vibriobactin synthetase is also unusual in that its NRPS machinery possesses two branch points. In a typical NRPS, the linear order of domains determines the final product [syringomycin synthetase from *Pseudomonas syringae* may present an exception: its final A domain appears to lie upstream of the first two modules (29)]. By contrast, in vibriobactin synthetase, the DHB-(S)-VibB acylated carrier is the first branch point; it serves as donor for both VibH (C domain) to acylate NSPD and for VibF (Cy₁ or Cy₂) to transfer to L-Thr and then to cyclize to the oxazoline (Figure 6). This product, 2-DHP-5-methyloxazoline-4-carboxyl-(S)-PCP on VibF, is the second branch point; it serves as donor for both subsequent acyl transfers to the remaining two amines of 7 (Figure 8).

Despite its characterization here as an oxazoline-forming NRPS competent for the final two acylations to produce vibriobactin, VibF still presents unusual aspects for further study. Foremost are the redundant cyclization domains: even though two condensation/heterocyclization events take place, both could be catalyzed by a single Cy domain, as the two L-Thr loadings are performed by one A domain. Second, the two C domains that flank the PCP domain in VibF are postulated to acylate the primary and secondary amines of DHB-NSPD sequentially. While we assume that both domains are active, mutagenesis will be necessary to assay each domain separately for competence and substrate specificity. In particular, C₁ has only weak homology to other NRPS C domains, and this only in the N-terminal half of the domain. Examination of this domain will assess the nonstandard core catalytic His motif as well as any obligatory ordering of the acylation events.

ACKNOWLEDGMENT

We are grateful to Joan R. Butters (Infectious Disease Division, Massachusetts General Hospital) for providing us with *V. cholerae* O395 genomic DNA. Preliminary sequence data for VibF from *V. cholerae* O1, strain N16961 was obtained from The Institute for Genomic Research website at <http://www.tigr.org>.

REFERENCES

- Griffiths, G. L., Sigel, S. P., Payne, S. M., and Neilands, J. B. (1984) *J. Biol. Chem.* 259, 383–385.
- Quadri, L. E. N. (2000) *Mol. Microbiol.* 37, 1–12.
- Gehring, A. M., Mori, I., and Walsh, C. T. (1998) *Biochemistry* 37, 2648–2659.
- Jalal, M. A. F., Hossain, M. B., van der Helm, D., Sanders-Loehr, J., Actis, L. A., and Crosa, J. H. (1989) *J. Am. Chem. Soc.* 111, 292–296.
- Cornish, A. S., and Page, W. J. (1995) *BioMetals* 8, 332–338.
- Yamamoto, S., Sugahara, T., Tougo, K., and Shinoda, S. (1994) *Microbiology* 140, 3117–3124.
- Yamamoto, S., Shinoda, S., Kawaguchi, M., Wakamatsu, K., and Makita, M. (1983) *Can. J. Microbiol.* 29, 724–728.
- Gehring, A. M., DeMoll, E., Fetherston, J. D., Mori, I., Mayhew, G. F., Blattner, F. R., Walsh, C. T., and Perry, R. D. (1998) *Chem. Biol.* 5, 573–586.
- Quadri, L. E. N., Keating, T. A., Patel, H. M., and Walsh, C. T. (1999) *Biochemistry* 38, 14941–14954.
- de Voss, J. J., Rutter, K., Schroeder, B. G., and Barry, C. E., III (1999) *J. Bacteriol.* 181, 4443–4451.
- Marahiel, M. A., Stachelhaus, T., and Mootz, H. D. (1997) *Chem. Rev.* 97, 2651–2673.
- Butterton, J. R., Choi, M. H., Watnick, P. I., Carroll, P. A., and Calderwood, S. B. (2000) *J. Bacteriol.* 182, 1731–1738.
- Wyckoff, E. E., Stoeber, J. A., Reed, K. E., and Payne, S. M. (1997) *J. Bacteriol.* 179, 7055–7062.
- Keating, T. A., and Walsh, C. T. (1999) *Curr. Opin. Chem. Biol.* 3, 598–606.
- Stein, T., Vater, J., Kruff, V., Otto, A., Wittmann-Liebold, B., Franke, P., Panico, M., McDowell, R., and Morris, H. R. (1996) *J. Biol. Chem.* 271, 15428–15435.
- Trucksis, M., Michalski, J., Deng, Y. K., and Kaper, J. B. (1998) *Proc. Natl. Acad. Sci. U.S.A.* 95, 14464–14469.
- Wyckoff, E. E., Valle, A.-M., Smith, S. L., and Payne, S. M. (1999) *J. Bacteriol.* 181, 7588–7596.
- Keating, T. A., Marshall, C. G., and Walsh, C. T. (2000) *Biochemistry* 39, 15513–15521.
- Keating, T. A., Miller, D. A., and Walsh, C. T. (2000) *Biochemistry* 39, 4729–4739.
- Heidelberg, J. F., Eisen, J. A., Nelson, W. C., Clayton, R. A., Gwinn, M. L., Dodson, R. J., Haft, D. H., Hickey, E. K., Peterson, J. D., Umayam, L., Gill, S. R., Nelson, K. E., Read, T. D., Tettelin, H., Richardson, D., Ermolaeva, M. D., Vamathevan, J., Bass, S., Qin, H., Dragoi, I., Sellers, P., McDonald, L., Utterback, T., Fleischmann, R. D., Nierman, W. C., White, O., Salzberg, S. L., Smith, H. O., Colwell, R. R., Mekalanos, J. J., Venter, J. C., and Fraser, C. M. (2000) *Nature* 406, 477–483.
- Konz, D., Klens, A., Schörgendorfer, K., and Marahiel, M. A. (1997) *Chem. Biol.* 4, 927–937.
- Stachelhaus, T., Mootz, H. D., Bergendahl, V., and Marahiel, M. A. (1998) *J. Biol. Chem.* 273, 22773–22781.
- Sankaranarayanan, R., Dock-Bregeon, A.-C., Rees, B., Bovee, M., Caillet, J., Romby, P., Francklyn, C. S., and Moras, D. (2000) *Nat. Struct. Biol.* 7, 461–465.
- Suo, Z., Walsh, C. T., and Miller, D. A. (1999) *Biochemistry* 38, 14023–14035.
- Gehring, A. M., Mori, I., Perry, R. D., and Walsh, C. T. (1998) *Biochemistry* 37, 11637–11650.
- Quadri, L. E. N., Sello, J., Keating, T. A., Weinreb, P. H., and Walsh, C. T. (1998) *Chem. Biol.* 5, 631–645.
- Weston, S. A., Camble, R., Colls, J., Rosenbrock, G., Taylor, I., Egerton, M., Tucker, A. D., Tunnicliffe, A., Mistry, A., Mancina, F., de la Fortelle, E., Irwin, J., Bricogne, G., and Pauptit, R. A. (1998) *Nat. Struct. Biol.* 5, 213–221.
- Wolf, E., Vassilev, A., Makino, Y., Sali, A., Nakatani, Y., and Burley, S. K. (1998) *Cell* 94, 439–449.
- Guenzi, E., Galli, G., Grgurina, I., Gross, D. C., and Grandi, G. (1998) *J. Biol. Chem.* 273, 32857–32863.
- Butterton, J. R., Stoeber, J. A., Payne, S. M., and Calderwood, S. B. (1992) *J. Bacteriol.* 174, 3729–3738.
- Butterton, J. R., and Calderwood, S. B. (1994) *J. Bacteriol.* 176, 5631–5638.